

1 Survival of the complex/Survival of the most flexible  
2 Tom Röschinger<sup>1</sup>, Simone Pompei<sup>2</sup>, Michael Lässig<sup>3,\*</sup>,  
3  
4  
5 1 Division of Chemistry and Chemical Engineering, California Institute of Technology, Pasadena,  
6 CA 91125  
7  
8 2 Institut für Biologische Physik, Universität zu Köln, Zülpicherstr. 77, 50937, Köln, Germany  
9 \* mlaessig@uni-koeln.de

## Abstract

### Introduction

The complexity of a system is a crucial component in molecular evolution. Evolution of gene regulation is often assumed to be driven by the gain and loss of transcription factor binding sites (TFBS), rather than the evolution of a transcription factor (TF) itself [1]. This assumption is based on the pleotropy of most TFs that have been observed, and that the pleotropic effects of a mutation in such a transcription factor are deleterious for most interactions, such that no change is possible. However, these TF's are conserved across species to begin with [2]. Some classes of TFs display extensive levels of species diversity while maintaining structure and function [3] and it has been discussed that protein evolution is a crucial source of developmental variation [4], but the consequences of protein evolution remain unclear [5, 6]. The evolution of gene regulatory networks is assumed to be driven by modifications and the evolution of TFs [7, 8].

## Methods

### Fitness Model

We are considering systems where the fitness is proportional to the binding of a single molecule to its functional site, such as a transcription factor to its operator. In thermodynamic equilibrium, the binding probability for this system is [9]

$$p_+(E) = \frac{1}{1 + e^{\beta(E - F_0)}}, \quad (1)$$

where  $F_0$  is the free energy of a random genome. This function has a sigmoid shape, which can approximated as an exponential function close to one of the plateaus. In analytical computations we often approximate high binding probability plateau as  $p_+(E) \sim (1 - e^{\beta(E - F_0)})$ . In addition, we consider the fitness effect of the binding site length. Generally, we assume that longer binding sites come with an increased fitness cost, since genome size is under selection especially in prokaryotes ([citation](#)). Therefore, we include a linear fitness cost  $f_l$  per position of the binding site to the system,

$$F(E, l) = f_0 p_+(E, l) - f_l l, \quad (2)$$

where  $f_0$  is the proportionality factor between binding probability to fitness. Note that the linear fitness cost for binding site length does not influence the dynamics of binding sites of fixed length, since the term maintains constant and selection coefficients are calculated as fitness differences, therefore canceling any constant additional term.

### Binding Energy Model

We assume a minimal energy model, where each position contributes independently to the total binding energy of the sequence, which is called the independent nucleotide approximation and

commonly used for Protein-DNA interactions [10, 11]. Therefore, we assume that minimal binding energy is achieved by a reference sequence, and each mismatch from that sequence brings a fixed cost to the binding energy of about  $\epsilon\beta \approx 2 - 3$  [9]. In this work we fix the energy cost per mismatch to be  $\epsilon\beta = 2$ , independent of the actual nucleotide at the position. For specific examples, there are methods to obtain real energy matrices that make it possible to compute the actual binding energy of a transcription factor to its binding site [12, 13].

Due to the linearity of the model, the total binding energy will increase with the length of the binding site, for both unspecific and specific sequences. We assume that the total number of unspecific binding site maintains constant, hence, the free energy difference  $\Delta E$  that is required to acquire specificity compared to off target binding sites maintains constant as well,

$$\Delta E = E_0(l) - E^*(l), \quad (3)$$

where we relabeled the free energy threshold in the sigmoid fitness landscape as  $E^*(l)$  and  $E_0(l) = 3/4l\epsilon$ , since a random sequence has  $1/4l$  just by chance. The free energy threshold is  $\Delta E = 10k_B T$  (argue either from minimal length of binding site or other source).

## Genetic Load and Length

One measure of adaption is the genetic load, which is computed as the difference of the mean fitness of a population to the maximal achievable fitness. Using the exponential approximation of the upper plateau of the binding term in the fitness landscape, the genetic load is simply given as the derivative of the fitness landscape evaluated at the mean energy  $\mathcal{L} = \beta|f'(\Gamma)|$  [14]. The time evolution of the trait mean is given by the stochastic equation

$$\dot{\Gamma} = m^\Gamma + \Delta_E f'(\Gamma) + \chi_\Gamma(t), \quad (4)$$

where  $m^\Gamma$  is the mutational drift,  $\Delta_E$  the diversity within a population regarding binding energy, and  $\chi_\Gamma(t)$  describes stochastic fluctuations.

## Mutation model

## Results

### Evolutionary Steady State in Non-equilibrium

This section should contain all necessary information and needs work on the language.

We start by investigating how externally driven mutations that change the consensus sequence of the binding site force the system into a new state that is different from the steady state that can be observed when binding is only disrupted by mutations in the binding site. Therefore, we use the Fokker-Planck equation describing the evolution of the mean  $\Gamma$  of a quantitative trait  $E$  [15],

$$\frac{\partial}{\partial t} Q(\Gamma, t) = \left[ \tilde{g}^{\Gamma\Gamma} \frac{\partial^2}{\partial \Gamma^2} - \frac{\partial}{\partial \Gamma} (m^\Gamma + \tilde{g}^{\Gamma\Gamma} \tilde{s}_\Gamma) \right] Q(\Gamma, t). \quad (5)$$

The equation can be broken down into three evolutionary forces: genetic drift, selection and mutations. In the low mutation rate regime, the selection term can be written as  $\tilde{s}_\Gamma = \partial_\Gamma f(\Gamma)$ , i.e., the derivative of the fitness landscape at the value of the trait mean. The effective diffusion coefficient is given by  $\tilde{g}^{\Gamma\Gamma} = \langle \Delta \rangle \sim \mu$  (include scaling with alphabet size here?), hence scaling the strength of selection with the variation of the trait within a population (mention Fisher's theorem here?). The mutational drift term is  $m^\Gamma = -\frac{n}{n-1}(\Gamma - \Gamma_0)$ , where  $n$  is the alphabet size of the binding site and  $\Gamma_0$  is the mean trait in the absence of selection. The mutation term describes deterministic drift that sites undergo due to mutations. If this term dominates the deterministic behavior, then most sites will have binding energies similar to random sequences. Driver mutations have the same impact on the binding energy as trailer mutations. Hence, in the evolutionary description of traits, we can add the driver mutation rate  $\rho$  to the trailer mutation rate  $\mu$  in the mutation term,  $m^\Gamma \sim -(\rho + \mu)(\Gamma - \Gamma_0)$ , for details see methods oder supplementary. The selection term  $\tilde{g}^{\Gamma\Gamma} \tilde{s}_\Gamma$  describes the selection coefficient of the trait mean value  $\tilde{s}_\Gamma$  and how it is amplified by the diversity within a population  $\tilde{g}^{\Gamma\Gamma} = \langle \Delta_E \rangle$ . For low mutation rates, the

diversity within a population is given by its value in the absence of selection, and very small.  
 Most positions are monomorphic, thus a mutation in the driver sequence changes the binding  
 energy for nearly all sites equally. Therefore, the diversity within a population is not affected by  
 driver mutations, and the selection term is invariant.

The non-deterministic term  $\tilde{g}^{\Gamma\Gamma}/2N$  describes how mutations lead to a spread in mean binding  
 energies across populations. In the original formulation this term also scales with the mean  
 diversity within a population. However, driver mutations also lead to an increased diversity across  
 populations, since they change the mean binding energy, while not effecting the mean diversity  
 within a population. Hence, we have to distinguish between the two response terms  $\tilde{g}^{\Gamma\Gamma}$ . The  
 response coefficient in the selection term, which only scales with the trailer mutation rate  $\mu$ , is  
 labeled  $\tilde{g}_s^{\Gamma\Gamma} \sim \mu$ . The response coefficient in the non-deterministic term is scaling with both  
 mutation rates and is labeled  $\tilde{g}_d^{\Gamma\Gamma} \sim \mu + \rho$ .

In the absence of selection, the steady state distribution  $Q_0(\Gamma)$  is the same as in the absence of  
 driving, since the scaling of both terms cancels out in the final solution ([Methods](#)). However, in a  
 driven environment  $\rho > 0$ , the steady state solution becomes

$$Q(\Gamma) = \frac{1}{Z} Q_0(\Gamma) \exp \left[ \frac{2N}{1+\kappa} F(\Gamma) \right], \quad (6)$$

where  $\kappa = \rho/\mu$  is the ration of driver and trailer mutation rate, which is the key parameter  
 describing the strength of non-equilibrium. A rescaling of the fitness landscape  $\hat{F}(\Gamma) = F(\Gamma)/(1+\kappa)$   
 reproduces the steady state distribution in equilibrium with a weaker fitness landscape. This result  
 is explained by the different scalings of the population genetic terms with non-equilibrium. The  
 mutation drift towards smaller binding energies increases as well as diffusion across populations,  
 while selection is not increased and therefore relatively weaker.

Note, that the rescaling of the fitness landscape effectively only applies to the term in the  
 fitness landscape regarding the binding probability. The fitness length cost is absorbed in the  
 normalization of the steady state distribution in 6. In the low mutation rate limit, an exact  
 steady state distribution can be numerically computed from substitution rates ([Methods](#) or  
[Supplementary](#)). In the regime of small selection coefficients  $Ns \sim 1$ , an analytic steady state  
 can be approximated ([Methods](#) or [Supplementary](#)), which is equal to the result in equation 6.

## Optimal Binding Site Length

In this section we discuss how the genetic load can be minimized by adapting the length of the  
 binding site in non-equilibrium. The genetic load is defined as the difference of the mean fitness  
 of the population to the maximum achievable fitness. ([Do we need a figure here?](#)). By minimzing  
 genetic load a population maximizes its fitness. In general increasing the length of genetic element  
 comes with a fitness cost, since more base pairs need to be kept specific to maintain function.  
 Therefore, we include a linear fitness cost to the fitness landscape ([Methods](#)). Note, this additional  
 fitness cost does not change dynamics when binding site lengths are kept constant because the  
 term cancels when computing selection coefficients. Non-equilibrium weakens the ability to find  
 specific binding sites, while the length fitness cost is independent of the state of the binding.  
 Hence, the fitness trade-off changes with the level of non-equilibrium. We can consider the fitness  
 effects in the terms of genetic load. For weak non-equilibrium most sites are functional and  
 are at the edge of the upper fitness plateau, which can approximated by an exponential tail.  
 Then the genetic load of a population is given by  $\mathcal{L} \sim |\frac{\partial}{\partial \Gamma} f(\Gamma, l)| + f_l l$ . The average load across  
 populations is given by the load at the deterministic mutation-selection balance  $\hat{\Gamma}$  ([Methods](#) or  
[Supplementary](#)) [14]. We retrieve two terms for the genetic load, with different scaling of the  
 binding length. The linear fitness cost for binding length, and the binding probability term with  
 scales inversely with binding length,

$$\mathcal{L} = \xi \frac{l_0}{l} (1 + \kappa) + \lambda \frac{l}{l_0} = \mathcal{L}_\kappa + \mathcal{L}_\lambda, \quad (7)$$

Where  $\xi$  is a combination of various parameters,  $\lambda = 2Nf_l/l_0 \sim 1$  is the scaled fitness cost  
 for length, and  $l_0$  is a length scaling parameter the derivation of this equation can be found in  
 the supplementary methods. Due to the trade off between the cost of adding positions to the

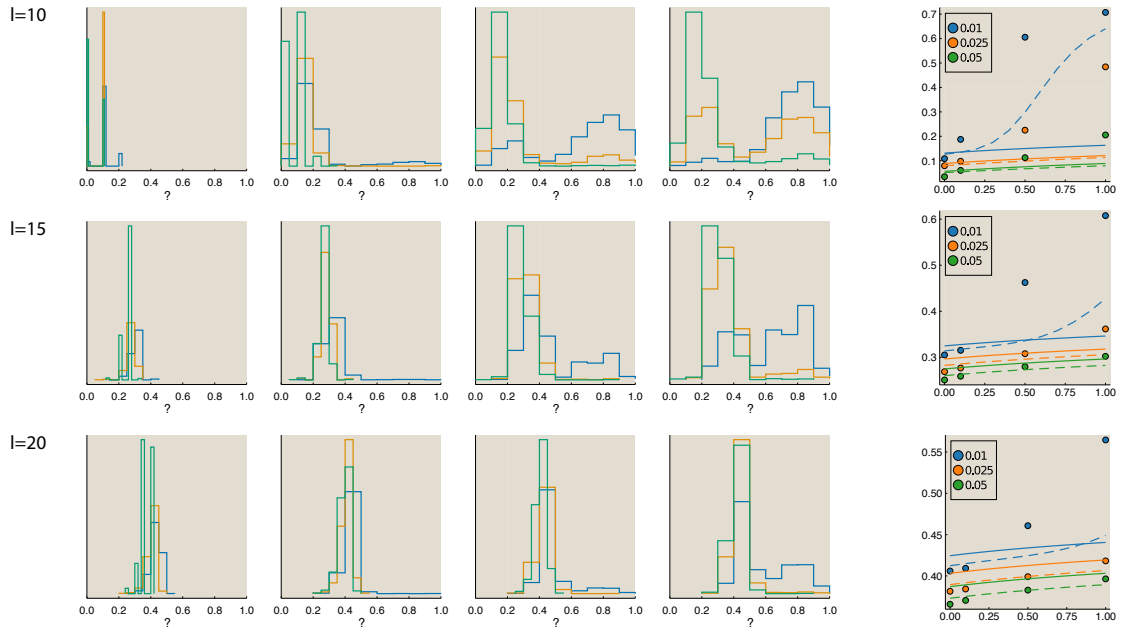


**Fig. 1.** Conceptual figure. Left side should show various distributions that evolved for fixed lengths at different fitness parameters  $f_0$  and how they change with increasing  $\kappa$ . For now, I simply plotted histograms, and the colors in each plot are the different fitness parameters (as seen in the legend on the right plot). Then, to show the distributions vary, we could show the mean (or peak) of each distribution on the right side and how it changes with increasing  $\kappa$ . This simulation was run **without recovery** of sites at the lower plateau, but is being repeated right now with recovery. This figure would support the first claim that the distribution in non-equilibrium can be written as the steady-state distribution with an additional factor of  $1/(1 + \kappa)$  in the exponent. Axis labels are going to be fixed in the next iteration.

binding site and reducing load by adding positions, there is an optimal binding site length, which minimizes the total genetic load,

$$l_{\text{opt}} \sim l_0 \sqrt{\frac{1 + \kappa}{\lambda}}. \quad (8)$$

Hence, we obtain a direct scaling of the optimal binding site length with non-equilibrium. The scaled fitness length cost in the model is chosen such that the binding site length in equilibrium ( $\kappa = 0$ ) is ten,  $l_{\text{opt}}(\kappa) = 0$ , which is the typical length of transcription factor binding sites [16].

## Dynamical Evolution of Binding Site Length

This section should be very descriptive, since it is one of the main results. And why considering the ratchet is important when writing down models of this kind which could consider binding site length. Also, could this be a reason for larger genomes, as soon as selection pressure decreases? Also, this section should have a minimal number of equations, just tell the story, and any computation should be in the supplementary methods, to make this section as straightforward to understand as possible.

In a real population, length adaptation is a dynamical process, driven by mutations which include a new position in the sequence in its recognition. We assume these mutations to be very rare compared to other type of mutations, such that the timescales separate. Therefore, we can assume that the system is in the respective steady state of binding energies each time a length mutation occurs. Assuming an alphabet size of  $n$  and using the match/mismatch energy model (see Methods), a newly added position will be a match with probability 1/4, since it has not been selected for yet and hence is random compared to the driver sequence. Length increase mutations are on average neutral in respect to the adaption term in the fitness landscape in first order, and are only influenced by the fitness cost of length (supplementary methods),

$$\sigma^+ = -\frac{\lambda}{l_0} = -\frac{\partial \mathcal{L}_\lambda}{\partial l}. \quad (9)$$

Since  $\lambda \sim 1$ , length increase mutations are in the regime of weak selection (Here either an explanation of what this means or a nice reference). However, length decrease mutations are affected by the fact that the binding site is adapted, i.e., removing a position is likely to hit an interaction which is beneficial to the binding interaction. If the binding site has  $k$  matches, then the probability of removing a match is  $k/l$ , which is much larger than the probability of adding a match, which we showed to be 1/4. The selection coefficient for removing a position has an additional term,

$$\sigma^- = \frac{\lambda}{l_0} - \xi \epsilon \beta \left( \frac{l_0}{l} \right)^2 (1 + \kappa) = \frac{\partial \mathcal{L}_\lambda}{\partial l} + l_0 \epsilon \beta \frac{\partial \mathcal{L}_\kappa}{\partial l}. \quad (10)$$

Unexpectedly, the adaptation term is scaled by the effective length scaling parameter, and the mutational effect. Therefore, the selection coefficient for length decrease mutations shows marginal selection,  $\sigma^- \sim (l/l_0)^2 \sim 1$ . Due to the separation of time scales, we can write down substitution rates for length mutations, which lead to a steady state distribution. In first order, we can compute the substitution rates as

$$u_{+-} \sim 1 + \frac{\sigma^{+/-}}{2} \sim \exp \left[ \frac{\sigma^{+/-}}{2} \right]. \quad (11)$$

Using detailed balance (Maybe avoid this term here?), we can compute the steady state distribution for binding site lengths. Using the rates above, we find that the resulting distribution is

$$P(l) \simeq \exp \left[ -\frac{\epsilon \beta l_0}{2} \mathcal{L}_\kappa - \mathcal{L}_\lambda \right]. \quad (12)$$

When comparing the maximum of this distribution with the length with minimizes the load, we find that the length  $l_{\text{opt}}^*$  which optimizes the effective potential resulting from the dynamical calculation is larger by a factor  $\sqrt{l_0}$ ,

$$l_{\text{opt}}^* = \epsilon \beta \sqrt{l_0} l_{\text{opt}}. \quad (13)$$

This is an enormous difference, see Figure (insert figure), and shows how important it is to consider the dynamics of the evolution of binding site lengths. Transcription factor binding sites have lengths around 10bp in prokaryotes (cite "Why are TF binding sites 10bp long."), so we can tune the fitness cost for length  $f_l$  such that the optimal length computed from the dynamical computation is around that value in equilibrium ( $\kappa = 0$ ). Then, we observe an increase in binding site length with increasing non-equilibrium, due to the sites being under more selective pressure to maintain their binding specificity, which shifts the weights in the trade off with the cost of increased binding site length.

171  
172  
173  
174  
175  
176  
177  
178

## Data

179  
180  
181

Placeholder for a possible section on some data. This has the lowest priority so far, and I think we should finish everything but the discussion before we dive into this.

## Discussion

182  
183  
184  
185  
186  
187  
188  
189

Here we should discuss the meaning of our results. The two factors of increased binding site length. First, the dynamics of length evolution lead to a much higher binding site length in equilibrium, than observed from minimizing the genetic load. But. Also we should discuss which data could support our theory. And finally, the shortcoming of the theory. Like how the approximation of the distribution is not really good for higher selection coefficients. And what how it could be used to improve. And finally how we think experiments could be set up to test the hypothesis experimentally.

190

## References

- [1] Murat Tugrul, Tiago Paixão, Nicholas H. Barton, and Gašper Tkačik. Dynamics of Transcription Factor Binding Site Evolution. *PLOS Genetics*, 11(11):e1005639, November 2015. Publisher: Public Library of Science.  
191  
192  
193
- [2] Dominic Schmidt, Michael D. Wilson, Benoit Ballester, Petra C. Schwalie, Gordon D. Brown, Aileen Marshall, Claudia Kutter, Stephen Watt, Celia P. Martinez-Jimenez, Sarah Mackay, Iannis Talianidis, Paul Flück, and Duncan T. Odom. Five-Vertebrate ChIP-seq Reveals the Evolutionary Dynamics of Transcription Factor Binding. *Science*, 328(5981):1036–1040, May 2010. Publisher: American Association for the Advancement of Science Section: Report.  
194  
195  
196  
197  
198
- [3] Katja Nowick and Lisa Stubbs. Lineage-specific transcription factors and the evolution of gene regulatory networks. *Briefings in Functional Genomics*, 9(1):65–78, January 2010. Publisher: Oxford Academic.  
199  
200  
201
- [4] Vincent J. Lynch and Günter P. Wagner. Resurrecting the Role of Transcription Factor Change in Developmental Evolution. *Evolution*, 62(9):2131–2154, 2008. eprint: <https://onlinelibrary.wiley.com/doi/10.1111/j.1558-5646.2008.00440.x>.  
202  
203  
204
- [5] Günter P. Wagner and Vincent J. Lynch. The gene regulatory logic of transcription factor evolution. *Trends in Ecology & Evolution*, 23(7):377–385, July 2008.  
205  
206
- [6] Karin Voordeckers, Ksenia Pougach, and Kevin J Verstrepen. How do regulatory networks evolve and expand throughout evolution? *Current Opinion in Biotechnology*, 34:180–188, August 2015.  
207  
208  
209
- [7] Irma Lozada-Chávez, Sarath Chandra Janga, and Julio Collado-Vides. Bacterial regulatory networks are extremely flexible in evolution. *Nucleic Acids Research*, 34(12):3434–3445, June 2006. Publisher: Oxford Academic.  
210  
211  
212
- [8] J. Christian Perez and Eduardo A. Groisman. Evolution of Transcriptional Regulatory Circuits in Bacteria. *Cell*, 138(2):233–244, July 2009.  
213  
214
- [9] Michael Lässig. From biophysics to evolutionary genetics: statistical aspects of gene regulation. *BMC Bioinformatics*, 8(6):S7, September 2007.  
215  
216

- 
- [10] Gary D. Stormo and Dana S. Fields. Specificity, free energy and information content in protein–DNA interactions. *Trends in Biochemical Sciences*, 23(3):109–113, March 1998. 217  
218
- [11] Marko Djordjevic. SELEX experiments: New prospects, applications and data analysis in inferring regulatory pathways. *Biomolecular Engineering*, 24(2):179–189, June 2007. 219  
220
- [12] Stephanie L. Barnes, Nathan M. Belliveau, William T. Ireland, Justin B. Kinney, and Rob Phillips. Mapping DNA sequence to transcription factor binding energy in vivo. *PLOS Computational Biology*, 15(2):e1006226, February 2019. 221  
222  
223
- [13] William T Ireland, Suzannah M Beeler, Emanuel Flores-Bautista, Nicholas S McCarty, Tom Röschinger, Nathan M Belliveau, Michael J Sweredoski, Annie Moradian, Justin B Kinney, and Rob Phillips. Deciphering the regulatory genome of *Escherichia coli*, one hundred promoters at a time. *eLife*, 9:e55308, September 2020. Publisher: eLife Sciences Publications, Ltd. 224  
225  
226  
227  
228
- [14] Torsten Held, Daniel Klemmer, and Michael Lässig. Survival of the simplest in microbial evolution. *Nature Communications*, 10(1):2472, June 2019. Number: 1 Publisher: Nature Publishing Group. 229  
230  
231
- [15] Armita Nourmohammad, Stephan Schiffels, and Michael Lässig. Evolution of molecular phenotypes under stabilizing selection. *Journal of Statistical Mechanics: Theory and Experiment*, 2013(01):P01012, January 2013. 232  
233  
234
- [16] Alexander J. Stewart, Sridhar Hannenhalli, and Joshua B. Plotkin. Why Transcription Factor Binding Sites Are Ten Nucleotides Long. *Genetics*, 192(3):973–985, November 2012. Publisher: Genetics Section: Investigations. 235  
236  
237
- [17] Motoo Kimura. On the probability of fixation of mutant genes in a population. *Genetics*, 47(6):713, 1962. Publisher: Genetics Society of America. 238  
239
- [18] Johannes Berg, Stana Willmann, and Michael Lässig. Adaptive evolution of transcription factor binding sites. *BMC evolutionary biology*, 4(1):42, 2004. Publisher: Springer. 240  
241

## Acknowledgments

242

## Author Contributions

243

## Competing Interests

244

The authors declare no competing interests.

245

---

<b>To Do List</b>	246
● Urgent:	247
– Michael: Supplementary Methods 3: Does the diversity within a population depend on the alphabet size, as seen from the analytic results? $\Delta E \sim \left(\frac{n}{n-1}\right)^2$ . This is important for the results in this section. Either mathematical proof or logical explanation.	248 249 250
– Tom: Think about loss at various fitness parameters, and how that relates to observable non-equilibrium.	251 252
– Tom: Get a first draft of the methods section ready so it is easy to refer to it when writing the results. The methods should not change too much anymore, unless we include data analysis, but this can be added later.	253 254 255
– Tom: Add conceptual figures (Optimal length scaling with non-equilibrium, effect of ratchet, two dimensional distribution $Q(\gamma, l)$ moving in 2D space with increasing $\kappa$ ).	256 257
● Remaining Tasks:	258
– Get all necessary simulations done and store results with README.md files to remember what they where.	259 260
– Finalize analytical computations in supplementary methods.	261
– Formulate punchline of the paper.	262
– Check references.	263
– Write introduction based on the results.	264
– Finalize results section.	265
– Spend one month looking for possible data sets.	266
– Either add data analysis or write discussion and be done.	267

---

**Comment 29. 7., edited 8. 9. Does the slow dynamics of  $\ell$  lead to a steady state that is localized at  $\ell_{\text{opt}}$ ?**

269

270

1. Our model has a conditional stationary distribution  $Q(k|\ell)$  peaked at  $k/\ell \equiv \gamma$  with

271

$$\gamma - \gamma_0 = \frac{\ell_0}{\ell} \quad (14)$$

and  $\gamma_0 = 1/4$ . This stationary state has a scaled load  $\mathcal{L} \equiv (F - F_{\max})/\tilde{\sigma}$  given by

272

$$\mathcal{L} = \mathcal{L}_\kappa + \mathcal{L}_\lambda = (\gamma - \gamma_0)(1 + \kappa) + \lambda \frac{\ell}{\ell_0}, \quad (15)$$

leading to an optimum length

273

$$\ell_{\text{opt}} = \ell_0 \sqrt{\frac{1 + \kappa}{\lambda}}. \quad (16)$$

2. In the exponential regime of the (scaled) fitness landscape  $\mathcal{F}(k|\ell) \equiv F(k|\ell)/\tilde{\sigma}$ , which is relevant for stable sites, the scaled load equals the scaled selection coefficient of site mutations,

274

275

276

$$s = \frac{\partial \mathcal{F}(k, \ell)}{\partial k} = \mathcal{L}_\kappa = (\gamma - \gamma_0)(1 + \kappa); \quad (17)$$

prefactors to be double-checked with Torsten-Daniel paper.

277

3. Perturbation theory in  $\epsilon \equiv 1/\ell_0$ . We can distinguish terms of order  $\epsilon$  and of order  $\ell/\ell_0 \sim 1$ . We have  $\gamma \sim \lambda \sim 1$  and  $\mathcal{L} \sim 1$ ; the scaling of  $\lambda$  follows from the requirement  $\ell_{\text{opt}} \approx \ell_0$  at  $\kappa = 0$ . In particular, we can distinguish selection coefficients  $\sim 1/\ell_0$  (weak selection) and  $\sim 1$  (marginal selection).

278

279

280

281

4. Adiabatic substitution dynamics of  $\ell$ . Length changes are assumed to occur with much smaller rates than mutations; we assume they are emitted from the steady state of the  $k$  dynamics. Each length change is coupled to a stochastic change of  $k$ . Because the dynamics takes place in the regime of weak and marginal selection, we use a linear approximation for substitution probabilities. Hence, we can first compute average selection coefficients  $\bar{s}_+$  and  $\bar{s}_-$  for changes of  $\ell$  and then evaluate the corresponding substitution rates using these averages.

282

283

284

285

286

287

288

In this framework, we find the processes  $\ell \rightarrow \ell + 1$  with average selection coefficient

289

$$\bar{s}_+ = \frac{3}{4} \frac{(-s)}{4} + \frac{1}{4} \frac{3s}{4} - \frac{\lambda}{\ell_0} \quad (18)$$

$$= -\frac{\lambda}{\ell_0} \quad (19)$$

(near-neutral evolution) and the processes  $\ell \rightarrow \ell - 1$  with average scaled selection coefficient

290

$$\bar{s}_- = \gamma \frac{(-3s)}{4} + (1 - \gamma) \frac{s}{4} + \frac{\lambda}{\ell_0} \quad (20)$$

$$= -(\gamma - \gamma_0)s + \frac{\lambda}{\ell_0} \quad (21)$$

$$= -(\gamma - \gamma_0)^2(1 + \kappa) + \frac{\lambda}{\ell_0} \quad (22)$$

$$= \ell_0 \frac{\partial \mathcal{L}_\kappa}{\partial \ell} + \frac{\partial \mathcal{L}_\lambda}{\partial \ell} \quad (23)$$

(marginal selection). These selection coefficients are of different magnitude: length increases are constrained only by the weak linear term, length decreases are marginally constrained by conservation of site function.

291

292

293

5. These asymmetric dynamics define an adaptive ratchet, which acts to increase selection for complexity. A typical cycle  $\ell \rightarrow \ell + 1 \rightarrow \ell$  has the following average scaled fitness balance:
- substitution  $\ell \rightarrow \ell + 1$ : weak fitness loss,  $\bar{s}_+ = -\lambda/\ell_0 = -O(\epsilon)$ ;
  - equilibration at  $\ell + 1$ : weak fitness gain,  $\Delta\mathcal{L}_{\ell+1} = \mathcal{L}_\kappa(\ell) - \mathcal{L}_\kappa(\ell + 1) \sim \ell_0/\ell^2 = O(\epsilon)$ ;
  - substitution  $\ell + 1 \rightarrow \ell$ : marginal fitness loss,  $\bar{s}_- = -\ell_0^2/\ell^2 = -O(\epsilon^0)$ ;
  - equilibration at  $\ell$ : marginal fitness gain,  $\Delta\mathcal{L}_\ell = -\mathcal{L}_\kappa(\ell) + \mathcal{L}_\kappa(\ell + 1) - \bar{s}_- = O(\epsilon^0)$ .

This cycle could inform a Figure.

6. Effective fitness landscape for length changes. We compute the ratio of the forward and backward substitution rate in first-order approximation,

$$\frac{u_{\ell \rightarrow \ell+1}}{u_{\ell+1 \rightarrow \ell}} = \frac{\exp(\bar{s}_+/2)}{\exp(\bar{s}_-/2)} + O(s^2) \quad (24)$$

$$\simeq \exp\left[-\frac{\ell_0}{2}(\mathcal{L}_\kappa(\ell + 1) - \mathcal{L}_\kappa(\ell)) - (\mathcal{L}_\lambda(\ell + 1) - \mathcal{L}_\lambda(\ell))\right] \quad (25)$$

$$\equiv \exp[\mathcal{F}_{\text{eff}}(\ell + 1) - \mathcal{F}_{\text{eff}}(\ell)] \quad (26)$$

with an effective scaled fitness potential

$$\mathcal{F}_{\text{eff}}(\ell) = -\frac{\ell_0}{2}\mathcal{L}_\kappa(\ell) - L_\lambda(\ell). \quad (27)$$

These rates define an equilibrium distribution

$$Q(\ell) \sim \exp[\mathcal{F}_{\text{eff}}(\ell)], \quad (28)$$

which is peaked at

$$\ell^* = \ell_0 \sqrt{\frac{\ell_0(1 + \kappa)}{2\lambda}} = \ell_{\text{opt}} \sqrt{\frac{\ell_0}{2}}. \quad (29)$$

Compared to the naive distribution  $Q(\ell) \sim \exp[-\mathcal{L}(\ell)]$ , which would lead to a peak at  $\ell_{\text{opt}}$ , the ratchet mechanism enhances the evolution of complexity.

## 7. Summary.

- Non-equilibrium weakens the selection on point mutations at a given complexity, as expressed by an effective fitness landscape

$$\mathcal{F}_{\text{eff}}(k|\ell) \sim \frac{1}{1 + \kappa}. \quad (30)$$

- Non-equilibrium introduces ratchet selection for complexity, as expressed by an effective fitness landscape

$$\mathcal{F}_{\kappa,\text{eff}}(\ell) \sim \ell_0(1 + \kappa). \quad (31)$$

This landscape is proportional to  $\ell_0$ ; that is, complexity begets more complexity.

## 8. Questions:

- (1) Is this in qualitative accordance with the evaluation of the rates in (26) beyond first order?
- (2) How does the fitness balance compare with the numerics?
- (3) How does  $\ell^*$  compare with the numerics?

## Comments 17. 12.

319

1. We could map the performance of the ratchet – in particular, the maximum complexity gain – as a function of the following independent parameters (see notebook adaptive ratchet 3):

- Binding free energy gap  $\Delta G$  (in units of  $k_B T$ ). Reasonable values:  $\Delta G \gtrsim 6$ .
- Functional binding length  $\ell_0$  (excess number of binding positions per site compared to average random sequence),

$$\ell_0 = \frac{\Delta G}{\epsilon_0}, \quad (32)$$

where  $\epsilon_0 = \Delta \Delta G$  is the average free energy effect per mutation. Reasonable values  $\epsilon_0 \sim 1$  (in units of  $k_B T$ ). Smaller  $\epsilon_0$  decrease curvature effects in the fitness landscape.

- Fitness effect per site,  $f_0$ . Reasonable values:  $f_0 \gtrsim 10$ . Smaller values of  $f_0$  increase the probability of function loss (in particular, at high  $\kappa$ ), larger values increase curvature effects in the fitness landscape.

The constraint selection coefficient  $\lambda$  is not independent, but is to be tuned so that equilibrium sites are close to the minimal functional length (to be implemented in notebook).

2. We know that sites tend to lose function at high  $\kappa$  and insufficient  $f_0$ . Can we analytically capture this effect by a condition for stability analogous to eq. (10) of the phenotypic interference paper? This would read

$$\frac{\mathcal{L}_b^*(\ell)}{\tilde{\sigma}} \lesssim \frac{f_0}{2} \quad (33)$$

with

$$\begin{aligned} \frac{\mathcal{L}_b^*(\ell)}{\tilde{\sigma}} &\equiv \frac{F_b(\gamma=1, \ell) - F_b(\gamma^*(\ell), \ell)}{\tilde{\sigma}} \\ &= \frac{(1+\kappa)(\gamma^*(\ell) - \gamma_0)}{\epsilon_0} \simeq \frac{(1+\kappa)\ell_0}{\epsilon_0 \ell}. \end{aligned} \quad (34)$$

3. A preliminary observation from the notebook is that the complexity gain appears to remain capped at about 2, even when the sites remain functional at the ML point. This seems to be caused by the length-increasing mutations becoming more negatively selected at higher values of  $\kappa$ . Can we understand why and maybe overcome this limit in some parameter regime?
4. Calibration of  $\lambda$ . Imposing the condition that the minimum functional site length equals the equilibrium length appears to give

$$\lambda = \frac{1}{\epsilon_0} \frac{\ell_0^2}{\ell_{\min}^2} \quad (35)$$

with  $\ell_{\min}(\gamma_0, \epsilon_0)$  given in the notebook. This expression is numerically too small and needs to be refined.

## Supplementary Information

345

### Supplementary Methods 1 Steady State Approximations

346

In the regime of low mutation rates,  $\mu N \ll 1$ , a population is in a monomorphic state, i.e., dominated by a single genotype, for most of the time. A new mutation fixes in the population with probability  $p(s)$  given by [17],

$$p(s) = \frac{1 - e^{-2s}}{1 - e^{-2Ns}}, \quad (36)$$

where  $s$  is the selection coefficient of the mutation and  $N$  the effective population size. Then, substitutions occur at a rate

$$u(s)_{E \rightarrow E'} = N\mu_{E \rightarrow E'} p(s), \quad (37)$$

where  $\mu_{E \rightarrow E'}$  is the rate at which a mutation occurs which changing the binding energy from  $E$  to  $E'$ . Here, we assumed that the fixation of a mutation is under selective pressure, which is the case for mutations in the trailer. We investigate the effects of mutations in the driver, which occur with rate  $\rho$ . These mutations are results of external events, e.g., a mutation in the coding sequence of a transcription factor leading to a missense mutation. In isolated system of driver and trailer, these mutations are not under selection pressure, but can change the binding energy nonetheless. Here we assume that these mutations happen for all driver sequences at the same time and therefore can be treated as substitutions as well. Thus, we add a term to the mutation rate in the form of

$$u(s)_{E \rightarrow E'} = N\mu_{E \rightarrow E'} p(s) + \rho_{E \rightarrow E'}, \quad (38)$$

where  $\mu_{E \rightarrow E'}$  is the mutation rate with driver mutations change the binding energy from  $E$  to  $E'$ . Assume, both trailer and driver have the same alphabet size, then both mutation rates are given by a constant rate times a factor accounting for the entropic difference between both states,  $\mu_{E \rightarrow E'} = \mu w_{E \rightarrow E'}$  and  $\rho_{E \rightarrow E'} = \rho w_{E \rightarrow E'}$ . Even if the assumption of equal alphabet sizes doesn't hold, e.g., in protein-DNA interaction, the differences in alphabet sizes can be accounted for by rescaling the mutation rates by a constant factor. The entropic term  $w$  is determined by the substitution rates in the absence of selection. We are looking for the distribution of binding energies at steady state, which is equivalent to

$$\frac{u(0)_{E \rightarrow E'}}{u(0)_{E' \rightarrow E}} = \frac{\mu_{E \rightarrow E'}}{\mu_{E' \rightarrow E}} = \frac{w_{E \rightarrow E'}}{w_{E' \rightarrow E}} = \frac{Q_0(E')}{Q_0(E)}, \quad (39)$$

where  $Q_0(E)$  is the distribution of binding energies in the absence of fitness. Even though there is non-equilibrium on the level of genotypes, we can look for a steady state distribution of the binding energies. Since the dynamics are one dimensional and fully described by the substitution rates, we can find the steady state distribution  $Q(k)$  by imposing detailed balance and solving

$$\frac{Q(E')}{Q(E)} = \frac{u(s)_{E \rightarrow E'}}{u(-s)_{E' \rightarrow E}} = \frac{N\mu_{E \rightarrow E'} p(s) + \rho_{E \rightarrow E'}}{N\mu_{E \rightarrow E'} p(s) + \rho_{E \rightarrow E'}}. \quad (40)$$

In equilibrium,  $\rho = 0$ , the fraction has an exact solution [18],

$$Q(k) = Q_0(k) \exp[2NF(k)]. \quad (41)$$

In non-equilibrium  $\rho > 0$ , the fraction does not simplify to an exact term as equation 41, but we can compute the exact steady state distribution numerically. However, in the limit of small selection coefficients  $Ns \sim 1$ , we can expand the fraction in orders of the selection coefficient and retrieve,

$$\begin{aligned} \frac{Q_0(E')}{Q_0(E)} \frac{N\mu p(s) + \rho}{N\mu p(s) + \rho} &\approx \frac{Q_0(E')}{Q_0(E)} \left[ 1 + \frac{2s(N-1)}{1 + \frac{\rho}{\mu}} + \frac{2s^2(N-1)^2}{(1 + \frac{\rho}{\mu})^2} + \mathcal{O}(s^3) \right], \\ &\approx \frac{Q_0(E')}{Q_0(E)} \exp \left[ \frac{2N}{1 + \kappa} F(E) \right]. \end{aligned} \quad (42)$$

---

Populations are usually large, so  $N - 1 \approx N$ , and up to second order the series is equal to an exponential function. The resulting distribution is therefore given by

375

376

$$Q(E) = Q_0(E) \exp \left[ \frac{2N}{1 + \kappa} F(E) \right]. \quad (43)$$

---

**Supplementary Methods 2 Scaling of Mutational Drift and Population Diversity with Alphabet Size and Driver mutations.**

377  
378  
379  
380  
381  
382  
383  
384

Here we use the population genetic notation of quantitative traits [15], and give a general form of the mutation drift. In addition we compute the contribution of driver mutations to the mutation drift.

The frequency of nucleotide  $i$  at locus  $k$  is given by  $y_k^i$ . The mutation drift of trailer mutations is therefore given by

$$m^\Gamma|_a = \sum_{k=1}^l \sum_{i>j}^n \mu_{j \rightarrow i} \Delta_{j \rightarrow i} (y_k^i - y_k^j), \quad (44)$$

where  $\mu_{j \rightarrow i}$  is the mutation rate from nucleotide  $j$  to nucleotide  $i$  and  $\Delta_{j \rightarrow i}$  is the energy difference of nucleotide  $j$  to  $i$ ,  $\Delta_{j \rightarrow i} = \epsilon_j - \epsilon_i$ . In the absence of any mutational bias, the mutation rates are equal,  $\mu_{j \rightarrow i} = \mu/n - 1$ , where  $\mu$  is the total mutation rate per position. Note that self mutations are excluded by definition. Inserting into the expression,

$$m^\Gamma|_a = \frac{\mu}{n-1} \sum_{k=1}^l \sum_{i>j}^n (\epsilon_k^j - \epsilon_k^i) (y_k^i - y_k^j), \quad (45)$$

we can multiply out the brackets to

$$m^\Gamma|_a = \frac{\mu}{n-1} \sum_{k=1}^l \left( (1-n) \sum_{j=1}^n \epsilon_k^j y_k^j + \sum_{i=1}^n \epsilon_k^i \sum_{j \neq i}^n y_k^j \right). \quad (46)$$

Now we use  $\sum_i y_k^i = 1$ , such that we can write  $\sum_{j \neq i} y_k^j = 1 - y_k^i$ ,

$$\begin{aligned} m^\Gamma|_a &= \frac{\mu}{n-1} \sum_{k=1}^l \left( (1-n) \sum_{i=1}^n \epsilon_k^i y_k^i + \sum_{i=1}^n \epsilon_k^i (1 - y_k^i) \right), \\ &= \frac{\mu}{n-1} \sum_{k=1}^l \left( -n \sum_{i=1}^n \epsilon_k^i y_k^i + \sum_{i=1}^n \epsilon_k^i \right). \end{aligned} \quad (47)$$

The mean trait value is given by  $\Gamma = \sum_{k=1}^l \sum_{i=1}^n E_i y_k^i$ , and the neutral mean value by  $\Gamma_0 = \frac{1}{n} \sum_{k=1}^l \sum_{i=1}^n E_i$ , therefore the mutation drift from trailer mutations is given by

$$m^\Gamma|_a = -\mu \frac{n}{n-1} (\Gamma - \Gamma_0) \quad (48)$$

In our model driver mutations occur as substitutions, therefore the nucleotide frequencies in the trailer do not change. In general, with the new driver element, each possible nucleotide at that position can have a different contribution to the binding energy. This difference is weighted with the allele frequency of each nucleotide. The energy of nucleotide  $i$  with driver element  $\alpha$  is denoted by  $E_i^\alpha$ , the energy at position before the mutation by  $E_i^*$ . The number of possible driver elements is given by  $\beta$ , and the mutation rate of driver element  $*$  to  $\alpha$  by  $\rho_{* \rightarrow \alpha}$ . Then the contribution to the mutation drift from driver mutations is given by

$$m^\Gamma|_b = \sum_{k=1}^l \sum_{\alpha=1}^{\beta} \sum_{i=1}^n \rho_{* \rightarrow \alpha} (E_i^\alpha - E_i^*) y_k^i. \quad (49)$$

Again, we assume that there is no mutational bias,  $\rho_{* \rightarrow \alpha} = \rho / (\beta - 1)$ . We can transform the sum to

$$\begin{aligned} &= -\frac{\rho}{\beta - 1} (\beta \Gamma - \sum_{k=1}^l \sum_{\alpha=1}^{\beta} \sum_{j=1}^n \epsilon_\alpha^j y_k^j), \\ &= -\rho \frac{\beta}{\beta - 1} (\Gamma - \Gamma'_0), \end{aligned} \quad (50)$$

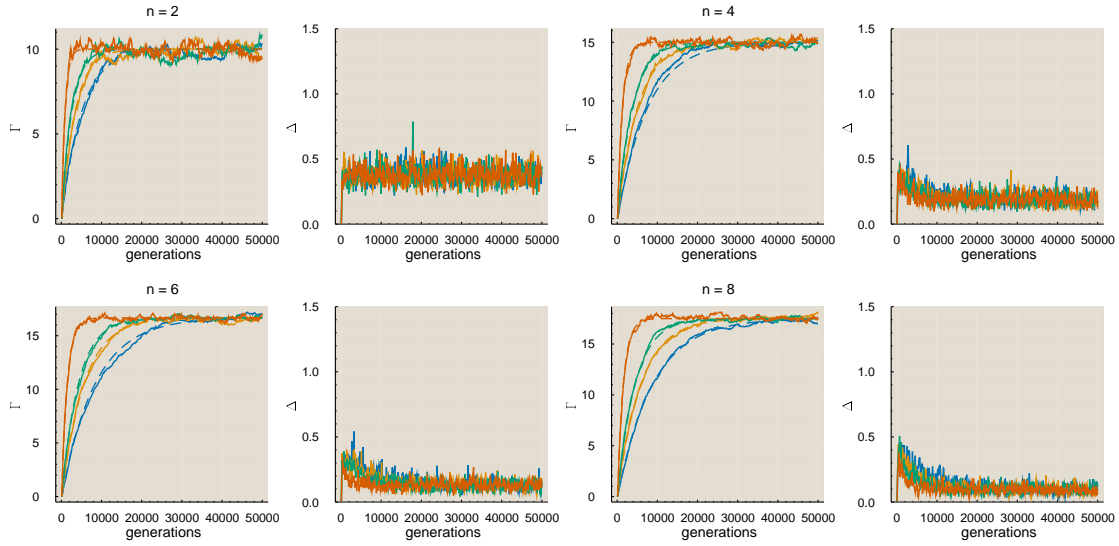


**Fig. 2.** Time evolution of mean and variance of populations in numeric simulations. Populations were initiated at  $\Gamma_i = 0$ , and run for 50000 generations with  $N = 1000$ ,  $\mu = 1/N$ ,  $l = 10$  and  $\kappa = 0, 0.5, 1, 5$  (blue, orange, green, red). Dashed lines show expected theoretical prediction.

where  $\Gamma'_0$  is the average over all possible binding energies with given trailer sequence. In general, this average is close to the neutral mean binding energy  $\Gamma_0$ . Then, the total mutation drift sums to

$$m^\Gamma = - \left( \mu \frac{n}{n-1} + \rho \frac{\beta}{\beta-1} \right) (\Gamma - \Gamma_0). \quad (51)$$

In the case if equal alphabet sizes of trailer and driver, the mutation drift takes the simple form

$$m^\Gamma = - \frac{n}{n-1} \mu (1 + \kappa) (\Gamma - \Gamma_0), \quad (52)$$

with the non-equilibrium parameter  $\kappa = \rho/\mu$ . If there are different alphabet sizes, then rescaling one of the mutation rates will give the same result. This result can be confirmed by numeric simulations by observing the time evolution of the mean energy of a population over time in the absence of fitness. Then, the deterministic (neglecting stochastic fluctuations) time evolution of the mean is given by

$$\dot{\Gamma} = m^\Gamma, \quad (53)$$

which has the analytical solution

$$\Gamma(t) = \Gamma_0 + (\Gamma_i - \Gamma_0) e^{-\frac{n}{n-1} \mu (1 + \kappa) t}. \quad (54)$$

In figure 2 we can see (add figure description).

In addition to the drift of the mean, we look at the scaling of the diversity within a population for various alphabet sizes and non-equilibrium ratios. From the simulations in figure 2, we already see that the diversity in steady state is the same for all tested non-equilibrium ratios. Since a substitution in the driver sequence changes the preferred nucleotide for each species, there is no significant change in the diversity within the population. To study the dependence on the alphabet size, we have to consider the effect mutation rate, that is the rate at which the binding energy changes, which differs if the alphabet is bigger than binary. Given that the total mutation rate per position is  $\mu$ , the trait changing mutation rate is also  $\mu$  if the position is a match, since any mutation will lead to a mismatch. However, if the position is a mismatch, then only one out of  $n - 1$  possible mutations leads to a trait change. Therefore, the average trait changing mutation rate  $\tilde{\mu}$  is given by

$$\tilde{\mu} = \frac{\Gamma}{\epsilon l} \frac{\mu}{n-1} + \left( 1 - \frac{\Gamma}{\epsilon l} \right) \mu. \quad (55)$$

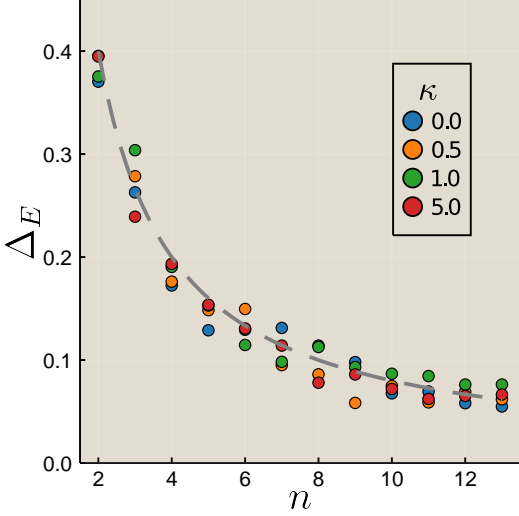


**Fig. 3.** Scaling of diversity within a population for various alphabet sizes and non-equilibrium ratios  $\rho = 0, 0.5, 1, 5$  (blue, orange, green, red). Dashed gray line shows theoretical prediction.

In the absence of fitness, the steady state mean binding energy is  $\Gamma/\epsilon = \Gamma_0\epsilon = 1 - 1/n$ , therefore the trait changing mutation rate is given by  $\tilde{\mu} = 2\mu/n$ . Then, the trait diversity within a population at steady state is given by

$$\Delta_E = \frac{2}{n}\mu N l \epsilon^2 \quad (56)$$

In figure 3 the diversity within populations is shown as a function of alphabet size. The endpoints from the same simulations shown in figure 2 fit the prediction well.

422  
423  
424

425  
426

### Supplementary Methods 3 Mutation-Selection-Balance and Non-Equilibrium.

427  
428  
429

The time evolution of the mean binding energy is given by [14]

$$\dot{\Gamma} = m^\Gamma + \Delta_E f'(\Gamma) + \chi_\Gamma(t), \quad (57)$$

with  $m^\Gamma = -\frac{n}{n-1}\mu(1+\kappa)(\Gamma - \Gamma_0)$  and  $\Delta_E = \frac{2\mu N l \epsilon^2}{n}$  (derived supplementary methods 2), where the mutation rate  $\mu$  is the absolute mutation per position. The mutation selection balance (MSB) is the deterministic fix point of this equation  $\dot{\Gamma}_{\text{MSB}} = 0$ . With the mutation drift from equation 52, we get

$$0 = -\frac{n}{n-1}\mu(1+\kappa)(\Gamma_{\text{MSB}} - \Gamma_0) + \frac{2\mu N l \epsilon^2}{n}f'(\Gamma_{\text{MSB}}). \quad (58)$$

Note that the MSB is invariant under the limit of a vanishing mutation rate  $\mu \rightarrow 0$ . At close to the upper plateau of the sigmoid fitness landscape the landscape can be approximated by an exponential landscape with derivative

$$\partial_\Gamma f(\Gamma, l) = -f_0\beta \exp[\beta(\Gamma - (\Gamma_0 - \Delta E))], \quad (59)$$

where  $\Gamma_0$  is the mean energy in a population in the absence of selection. In the model of matches and mismatches, this is simply  $\Gamma_0 = \epsilon 3l/4$  in a four letter alphabet, where  $\epsilon$  is the energy contribution of a mismatch.

Then, we can rewrite equation 58 to retrieve the transcendental equation

$$\Gamma_{\text{MSB}} = \Gamma_0 + \frac{(n-1)}{n^2} \frac{1}{1+\kappa} 2Nl\epsilon^2 \beta \exp[-\beta(\Gamma_{\text{MSB}} - (\Gamma_0 - \Delta E))], \quad (60)$$

which is solved by the ProductLog,

$$\Gamma_{\text{MSB}}(l) = \Gamma_0 - \frac{1}{\beta} \text{ProductLog}\left(\frac{n-1}{n^2} \frac{2Nf_0l\epsilon^2\beta^2 e^{\beta\Delta E}}{1+\kappa}\right). \quad (61)$$

We can rewrite this result in terms of relative number of mismatches  $\gamma/\epsilon l$ ,

$$\gamma_{\text{MSB}}(l) - \gamma_0 = -\frac{1}{l\epsilon\beta} \text{ProductLog}\left(\frac{n-1}{n^2} \frac{2Nf_0l\epsilon^2\beta^2 e^{\beta\Delta E}}{1+\kappa}\right). \quad (62)$$

Although the ProductLog scales with the binding site length  $l$  and the non-equilibrium ratio  $\kappa$ , we can treat it as a constant,

$$l_0 = \frac{1}{\beta\epsilon} \text{ProductLog}\left(\frac{n-1}{n^2} \frac{2Nf_0l\epsilon^2\beta^2 e^{\beta\Delta E}}{1+\kappa}\right). \quad (63)$$

Now we can write

$$\gamma_{\text{MSB}}(l) - \gamma_0 \approx -\frac{l_0}{l}. \quad (64)$$

Having equation (61) in hand, we can solve equation (58) for the fitness derivative at the Mutation-Selection-Balance,  $f'(\Gamma_{\text{MSB}}(l)) = \hat{f}(l)$ ,

$$\hat{f}(l) = -\frac{1}{\epsilon(n-1)} \frac{n^2}{2Nl} \frac{1+\kappa}{l} l_0. \quad (65)$$

In the exponential fitness landscape, the scaled genetic load is given by the derivative of the fitness landscape in respect of the energy and the length fitness cost,

$$\mathcal{L} = 2N \left( -\frac{f'(\Gamma)}{\beta} + f_l l \right). \quad (66)$$

Also we know, that the deterministic load is equal to the average load,

$$\mathcal{L} = 2N \left( -\frac{\hat{f}(l)}{\beta} + f_l l \right) \quad (67)$$

Finally, we can write the genetic load as a function of the driving parameter  $\kappa$  and the binding length,

$$\mathcal{L}(l, \kappa) = \frac{n^2}{n-1} \frac{1+\kappa}{\beta\epsilon} \frac{l_0}{l} + \lambda \frac{l}{l_0}, \quad (68)$$

with the scaled fitness cost  $\lambda = 2Nf_l/l_0$ . This load is minimized for given parameters at length

$$l_{\text{opt}} = l_0 \sqrt{\frac{n^2}{\epsilon\beta\lambda(n-1)}(1+\kappa)}. \quad (69)$$

The parameter  $\lambda$  can be found by fixing the optimal length in equilibrium  $l_{\text{opt}}(\kappa=0) = 10$ .

451  
452  
453  
454

---

## Supplementary Methods 4 Dynamical Length Evolution.

455  
456  
457  
458  
459  
460

The slow dynamics of binding site length evolution leads to an asymmetry. As shown in equation (64), the conditional stationary distribution  $Q(k|l)$  is peaked at  $\gamma \approx \gamma_0 - l_0/l$ . We compute the selection coefficients of length mutations in first order, using the expansion of the exponential fitness landscape

$$F(\Gamma, l) = F(\Gamma', l') + (\Gamma - \Gamma')f'(\Gamma', l') + (l - l')\left(\frac{n-1}{n}\epsilon f'(\Gamma', l') - f_l\right), \quad (70)$$

where we used  $f'(\Gamma', l') = \partial_\Gamma F(\Gamma', l') = n/(n-1)\epsilon \partial_l F(\Gamma', l')$ . The selection coefficients for length mutations are the given by,

$$s_+^M = F(\Gamma, l+1) - F(\Gamma, l) = -f_l - \frac{n-1}{n}\epsilon f'(\Gamma, l), \quad (71)$$

$$s_+^{MM} = F(\Gamma + \epsilon, l+1) - F(\Gamma, l) = -f_l + \frac{1}{n}\epsilon f'(\Gamma, l), \quad (72)$$

$$s_-^M = F(\Gamma, l) - F(\Gamma, l+1) = f_l + \frac{n-1}{n}\epsilon f'(\Gamma, l), \quad (73)$$

$$s_-^{MM} = F(\Gamma - \epsilon, l) - F(\Gamma, l+1) = f_l - \frac{1}{n}\epsilon f'(\Gamma, l), \quad (74)$$

where the subscript is indicating increase (+) or decrease mutation (-) and the superscript is indicating whether the mutation is regarding a match( $M$ ) or mismatch( $MM$ ). When adding a position, a match is added with probability  $1/n$ , and mismatch with probability  $(n-1)/n$ . The average selection coefficient of a length increase mutation is then given by

$$\bar{s}_+ = \frac{1}{n}s_+^M + \frac{n-1}{n}s_+^{MM} = -f_l. \quad (75)$$

When removing a position, the probability of removing a match is equal to the ratio of matches in the binding site  $1 - \gamma$ , hence the average selection coefficient for a decrease mutation is given by

$$\bar{s}_- = \gamma s_-^{MM} + (1 - \gamma)s_-^M = f_l - (\gamma - \gamma_0)f'(\Gamma, l)\epsilon. \quad (76)$$

Now we can insert equations (64) and (65). Then, the scaled selection coefficients  $\sigma = 2Ns$  are given by

$$\sigma_+ = -\frac{\lambda}{l_0}, \quad (77)$$

$$\sigma_- = \frac{\lambda}{l_0} - \left(\frac{l_0}{l}\right)^2 \frac{n^2}{n-1}(1+\kappa). \quad (78)$$

Here we can see the asymmetry of length mutations. Length increase mutations are only constrained by the small fitness cost of each position, with  $\sigma_+ \sim 1/l_0$  (near-neutral evolution), while length decrease mutations are marginally constrained by conservation of site function with  $\sigma_- \sim l_0^2/l^2 \sim 1$  (marginal selection). We can write the selection coefficients as derivatives of the load,

$$\sigma_+ = -\frac{\partial \mathcal{L}_l}{\partial l}, \quad (79)$$

$$\sigma_- = -\epsilon \beta l_0 \frac{\partial \mathcal{L}_\kappa}{\partial l} + \frac{\partial \mathcal{L}_l}{\partial l}. \quad (80)$$

Due to the separation of timescales, we can compute a steady state distribution of binding lengths  $P(l)$ . This distribution is obeying detailed balance, therefore we can compute

$$\frac{P(l)}{P(l+1)} = \frac{u_-(l+1)}{u_+(l)}, \quad (81)$$

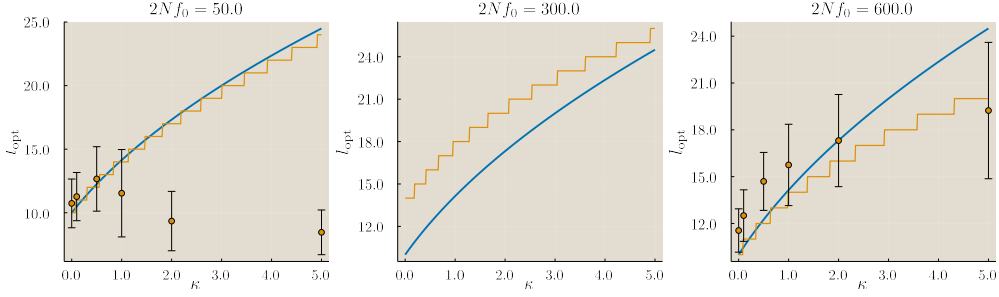


**Fig. 4.** Optimal length for varying maximal fitness values. Blue is predicted curve, orange dots are simulations from substitution dynamics. Error bars are standard deviation from the mean.

where  $u_+$  is the length increase substitution rate and  $u_-$  is the length decrease mutation rate. In first order we can rate the ratio of the to rates as

$$\frac{u_-(l+1)}{u_+(l)} = \frac{\exp(\sigma_+/2)}{\exp(\sigma_-/2)} + \mathcal{O}(\sigma^2), \quad (82)$$

$$\simeq \exp \left[ -\frac{\epsilon \beta l_0}{2} (\mathcal{L}_\kappa(l+1) - \mathcal{L}_\kappa(l)) - (\mathcal{L}_\lambda(l+1) - \mathcal{L}_\lambda(l)) \right], \quad (83)$$

$$= \exp [\mathcal{F}_{\text{eff}}(l+1) - \mathcal{F}_{\text{eff}}(l)], \quad (84)$$

which the scaled effective potential

469

$$\mathcal{F}_{\text{eff}}(l) = -\frac{\epsilon \beta l_0}{2} \mathcal{L}_\kappa(l) - \mathcal{L}_\lambda(l). \quad (85)$$

These rates define an equilibrium distribution

470

$$Q(l) \sim \exp [\mathcal{F}_{\text{eff}}(l)], \quad (86)$$

which is peaked at

471

$$l_{opt} = l_0^{3/2} \sqrt{\frac{n^2}{2\lambda(n-1)}(1+\kappa)}. \quad (87)$$